Research article

Spectrum of chest computed tomographic (CT) findings in coronavirus disease-19 (COVID-19) patients in India

Arshed Hussain Parry[a], Abdul Haseeb Wani[b,*], Mudasira Yaseen[c], Khurshid Ahmad Dar[d], Naseer Ahmad Choh[a], Naseer Ahmad Khan[b], Naveed Nazir Shah[d], Majid Jehangir[b]

[a] Department of Radiodiagnosis, Sher-i-Kashmir Institute of Medical Sciences, Srinagar, Jammu & Kashmir, India
[b] Department of Radiodiagnosis, Government Medical College, Srinagar, Jammu & Kashmir, India
[c] Department of Anesthesiology and Critical Care Medicine, Sher-i-Kashmir Institute of Medical Sciences, Srinagar, Jammu & Kashmir, India
[d] Department of Respiratory Medicine, Chest Disease Hospital, Srinagar, Jammu & Kashmir, India

ABSTRACT

Purpose: To report the spectrum of chest computed tomographic (CT) imaging findings in coronavirus disease-19 (COVID-19) infected Indian patients.
Methods: This was a prospective descriptive study comprising 147 consecutive reverse transcriptase polymerase chain reaction (RT-PCR) positive patients who underwent CT chest. Prevalence, distribution, extent and type of abnormal lung findings were recorded.
Results: Among the total study cohort of 147 patients, 104 (70.7 %) were males and 43 (29.3 %) were females with mean age of 40.9 ± 17.2 years (range 24–71 years). We observed lung parenchymal abnormalities in 51 (34.7 %) cases whereas 96 (65.3 %) RT-PCR positive cases had a normal chest CT. Only 12.2 % of the patients were dyspneic, 6.1 % had desaturation, 7.4 % had increased respiratory rate and 10.9 % had comorbidities. Among the patients with abnormal CT findings bilateral 39/51 (76.5 %), multilobar (88.2 %) lung involvement with a predominant peripheral and posterior distribution was commonly observed. With regards to the type of opacity, ground glass opacity (GGO) was the dominant abnormality found in all 51 (100 %) cases. Pure GGO was observed in 15 (29.4 %), GGO with crazy paving pattern was seen in 15 (29.4 %) and GGO mixed with consolidation was noted in 21(41.2 %). Peri-lesional or intralesional segmental or subsegmental pulmonary vessel enlargement was observed in 36 (70.6 %) cases.
Conclusion: In this study population predominantly with mild symptoms and few comorbidities, two-thirds of RT-PCR positive patients had a normal chest CT; whereas the remaining patients showed typical findings of predominant GGOs with a bilateral distribution and peripheral predominance.

1. Introduction

Coronavirus disease 2019 (COVID-19), caused by severe acute respiratory syndrome coronavirus 2 (SARS-CoV-2) has spread unabated across the globe after its emergence in Wuhan, China at the end of 2019. According to the World Health Organisation (WHO) situation report-137 more than 6.5 million people have confirmed positive globally with 387 177 deaths as of June 05, 2020 [1].

SARS-CoV-2 is an enveloped single-stranded RNA virus [2,3]. The clinical presentation ranges from asymptomatic, mildly symptomatic cases to severely ill [4,5]. Imaging findings of COVID-19 closely resemble other viral pneumonias and mainly include ground glass opacities (GGO) with a peripheral and basal predominance as the initial

manifestation of the disease [6]. There is a gradual transformation of GGOs into consolidations during the intermediate stage of the disease. The CT findings peak around 9–13 days after symptom onset. Clinical recovery is associated with a gradual resorption of pulmonary opacities with development of subpleural lines, reticulations, fibrous stripes and perilobular opacities, usually apparent after the second week. In some patients the clinical course is complicated by acute respiratory distress syndrome (ARDS) or pulmonary embolism, the main causes of death [6]. Pleural effusion, pericardial effusion, mediastinal lymphadenopathy are seen in patients with severe disease [7,8].

The aim of the present study was to report the chest CT imaging manifestations of SARS-CoV-2 infection in Kashmir, India.

---

* Corresponding author.
  E-mail address: soberseeb@gmail.com (A.H. Wani).

2. Material and methods

2.1. Patient cohort and study design

This was a prospective observational study from 17, March 2020 to 16, April 2020, conducted in our hospital in Kashmir, India, which was a designated COVID-19 Care Centre (CCC) with separate inpatient, intensive care unit (ICU) and quarantine facilities. Requirement of informed patient consent was waived off by the Institutional Ethical Committee (IEC). 147 consecutive symptomatic patients referred to our CCC from various districts were subjected to chest CT after obtaining nasopharyngeal swab for RT-PCR.

2.1.1. Inclusion criteria

Patients with symptoms such as fever, cough, fatigue, sore throat and/or dyspnea with RT-PCR confirmed SARS-CoV-2 infection.

2.1.2. Exclusion criteria

Asymptomatic patients with RT-PCR confirmed SARS-CoV-2 infection.

Clinical characteristics including age, gender, history of exposure, symptoms, blood tests including complete blood count (CBC) and C-reactive protein (CRP) and outcome data during the hospital stay were collected and analyzed.

Patients with severe illness, defined by the WHO interim guidelines for clinical management of COVID-19 as [a] respiratory rate $\geq$ 30 breaths/min, or [b] oxygen saturation (SpO2) $\leq$ 90 %, or [c] respiratory failure needing mechanical ventilation, or [d] ARDS, or [e] shock [9] were admitted to intensive care unit (ICU). Patients with symptoms but no signs of respiratory failure were admitted in routine ward. Asymptomatic cases did not undergo chest CT and were observed in the quarantine facility of the CCC.

2.2. CT acquisition protocol

Chest CT was performed on an average 5.8 days (range 3–9 days) after symptom onset. Non-contrast chest CT was performed using a 16-row multi-detector CT unit (SOMATOM Emotion 16 scanner; Siemens, Erlangen, Germany) with the following parameters: tube voltage 100–120 kVp, tube current 90–130 mA s, collimation of 16 × 0.6 and a pitch of 1.5. The CT images were acquired in a single inspiratory breath-hold. Images were reconstructed using increment of 0.7 mm into 1 mm thick slices. The images were viewed in both lung window settings (width 1200–1500 HU; centering -500 to -600HU) and mediastinal window (width 300 − 400HU; centering 40HU). Decontamination of the CT suite was performed using 70 % ethanol or 0.1 % sodium hypochlorite. After each CT examination, passive air exchange was allowed for 60 min.

2.3. Image analysis

Two radiologists (P.A, WA with 8 and 7 years of experience in radiology, respectively) independently reviewed CT images on an Osirix MD workstation (Apple Mac) [10]. In case of any disagreements between the two primary interpreting radiologists, two senior radiologists (J.M and C.N with 18 and 15 years of experience, respectively) adjudicated the final decision. The readers assessed the following features: presence or absence of pulmonary opacities; location; type of opacities and the extent of opacities.

The location of lesions was specified with regards to involvement of one lung (right, left) or both the lungs. The number of lobes involved was determined. Zonal distribution of the opacities was classified as central (defined as the inner two-third of the lung tissue) and peripheral (defined as outer one-third of the lung). The distribution of lung abnormalities was also dichotomized into anterior and posterior location (lung tissue anterior to a line drawn midway on axial CT was defined as

anterior and the portion behind it was defined as posterior). Lung lesions were categorized using Fleischner society glossary of terms for thoracic imaging [11]. GGO (ground glass opacity) was defined as an increase in the density of lung with non-obscuration of bronchial and vascular structures, whereas consolidation was defined as increased density of lung tissue through which vascular and bronchial structures were not visible. Furthermore, the readers also evaluated presence of associated airway, vascular, pleural and mediastinal abnormalities. A semi-quantitative scoring system was used to quantitatively estimate the pulmonary involvement by visually calculating the percentage of the total lung involvement by dividing each lung into 3 zones, followed by averaging the 6 zones to obtain the percentage of the total lung involvement [12].

2.4. Statistical analysis

Statistical analysis was performed using the Statistical Package for the Social Sciences (SPSSInc. Chicago, IL, version 21.0). Continuous variables were expressed as mean, ranges and standard deviation, whereas categorical variables were expressed as counts and percentages. The agreement between two interpreting radiologists for CT findings was evaluated with the Kappa method (according to Landis and Koch 0: poor agreement; 0.01 − 0.20: slight agreement; 0.21 − 0.40: fair agreement; 0.41 − 0.60: moderate agreement; 0.61 − 0.80: substantial agreement; 0.81–1.0: almost perfect agreement).

3. Results

3.1. Demographics, clinical characteristics and laboratory findings

Among the total study cohort of 147 patients, 104 (70.7 %) were males and 43 (29.3 %) were females with mean age of 40.9 ± 17.2 years (range 24–71 years). In 141 (95.9 %) cases a history of close contact with an infected patient or a history of travel to a high risk zone within or outside the country was forthcoming. Fever was the commonest symptom seen in 74 (50.3 %) followed by fatigue or malaise in 61 (41.4 %), cough in 57(38.8 %) and sore throat in 41 (27.9 %). Only 18 (12.2 %) of the patients were dyspneic, 11 (7.4 %) had increased respiratory rate and 9 (6.1 %) had desaturation. Comorbidities were present in 16 (10.9 %) patients. Lymphopenia was observed in 50 (34 %) patients whereas lymphocytosis was seen in 14 (9.5 %). C-reactive protein was elevated in 77 (52.4 %) patients. Patient demographics, clinical features and laboratory investigations are summarized in Table 1.

3.2. Chest CT findings

There was almost a perfect agreement (Cohen's Kappa of 0.83) in reading CT images between the two primary radiologists. The result of chest CT along with the clinical course of study cohort is depicted in Fig. 1.

Lung parenchymal abnormalities were observed in 51 (34.7 %) cases, whereas 96 (65.3 %) RT-PCR positive cases had a normal chest CT. Among the patients with abnormal CT findings, bilateral lung involvement was the commonest, observed in 39/51 (76.5 %). Multiple lobe involvement was seen more frequently. 24 (47.1 %) had involvement of all the 5 lobes whereas two lobe and single lobe involvement was seen in 6 (11.8 %) each. In terms of axial distribution, peripheral distribution was the commonest, seen in 51 (100 %) cases among which 36 (70.6 %) had only peripheral distribution whereas as 15 (29.4 %) had both peripheral and central distribution. None of the patients showed purely central distribution. Similarly, with regards to the anterior-posterior distribution all the 51(100 %) cases had posterior distribution of lung findings among which 27 (52.9 %) had only posterior distribution whereas 24 (47.1 %) had combined posterior and anterior distribution with none of the cases showing solitary anterior

Table 1

Demographics, Clinical characteristics and Laboratory data for COVID-19 infected patients.

Patient demographics	Number of patients (n = 147)	%
Mean age(years) ± S.D	40.9 ± 17.2	
Gender		
Male	104	70.7
Female	43	29.3
History of contact with a COVID-19 patient or travel to a high risk zone		
Present	141	95.9
Absent	6	4.1
Co-morbid illness		
Hypertension	9	6.1
Diabetes Mellitus	5	3.4
CLD	1	0.7
Rheumatoid Arthritis	1	0.7
Clinical features		
Fever	74	50.3
Cough	57	38.8
Sore throat	41	27.9
Dyspnea	18	12.2
Malaise/Fatigue	61	41.4
Increased Respiratory rate (> 30 /min)	11	7.4
Reduced Oxygen Saturation (< 90%)	9	6.1
Lab Investigations		
Mean WBC count (normal value 4-11 $\times 10^9$ /L)	5.3	
Lymphocyte count (normal value 1.1-3 $\times 10^9$ /L)		
Increased	14	9.5
Decreased	50	34
Increased CRP (normal value < 10 mg/L)	77	52.4

CLD-Chronic liver disease; WBC- white blood cells; CRP- C-reactive protein.

Table 2

Distribution of lung findings on chest CT.

Lung parenchymal abnormalities on CT	Number of patients	%
Present	51	34.7
Absent	96	65.3
Laterality of lung involvement		
Bilateral	39	76.5
Right lung	6	11.8
Left lung	6	11.8
Lobar involvement		
Right upper lobe	45	88.2
Right middle lobe	30	58.8
Right lower lobe	39	76.5
Left upper lobe	42	82.4
Left lower lobe	39	76.5
Number of lobes involved		
5 lobes	24	47.1
4 lobes	12	23.5
3 lobes	3	5.8
2 lobes	6	11.8
1 lobe	6	11.8
Axial location of opacity		
Central (inner 2/3rd of lung)	0	0
Peripheral (outer 1/3rd of lung)	36	70.6
Central and Peripheral	15	29.4
Antero-posterior location		
Anterior	0	0
Posterior	27	52.9
Anterior and posterior	24	47.1

distribution. The laterality and distribution of lung abnormalities is given in Table 2. With regards to the type of opacity, GGO was the dominant abnormality, found in all 51 (100 %) cases. Pure GGO was observed in 15 (29.4 %), GGO with interlobular septal thickening and intralobular lines, producing crazy paving pattern was seen in 15 (29.4 %) and GGO mixed with consolidation was noted in 21(41.2 %) (Figs. 2 and 3). None of the patients showed pure consolidation. Reticulations were seen in 15 (29.4 %) (Fig. 4). A small number of cases showed subpleural curvilinear lines (17.6 %) (Fig. 4), air bronchogram sign (23.5 %) and atoll or reverse halo sign (17.6 %) (Fig. 3). Bronchial wall thickening was observed in 6 (11.9 %) and bronchodilatation was seen in 3 (5.9 %). We observed peri-lesional or intralesional segmental or subsegmental vessel enlargement in 36 (70.6 %) cases (Fig. 5). None of the patients showed halo sign or cavitation. None of the patients showed pleural effusion, pericardial effusion or mediastinal lymphadenopathy. A higher percentage of diseased lung was observed in patients with severe disease requiring ICU admission (29.6 ± 12.3 %) (mean ± SD) than in-ward patients with a mild form of disease (10.2 ± 6.6 %) (mean ± SD). Of the 51 CT positive cases, 6 (11.7 %) were admitted in ICU. Two of them demised (one had underlying diabetes and one had chronic liver disease). Only one patient among the negative CT group developed respiratory worsening 9 days after symptom onset and required ICU admission. However, the patient survived.

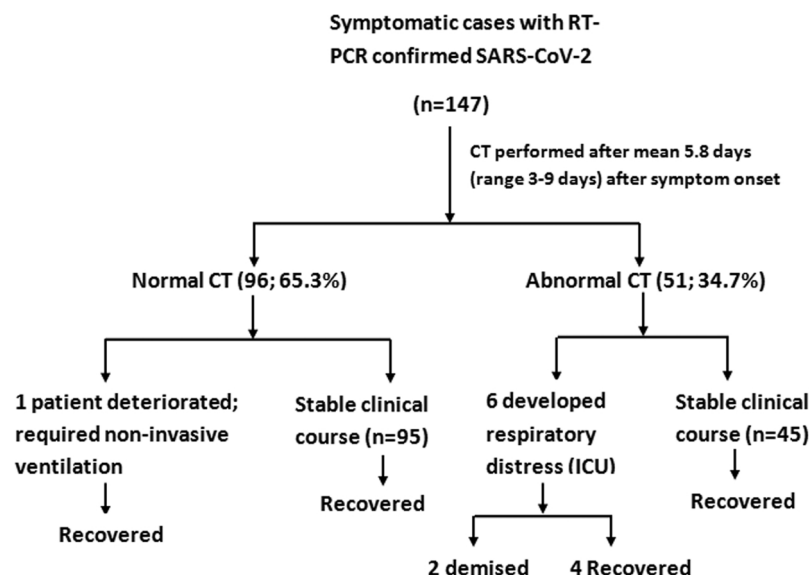Lung parenchymal abnormalities are summarized in Table 3.

Fig. 1. Flow chart depicting the result of chest CT in symptomatic RT-PCR confirmed SARS-CoV-2 infected patients along with the clinical outcome.
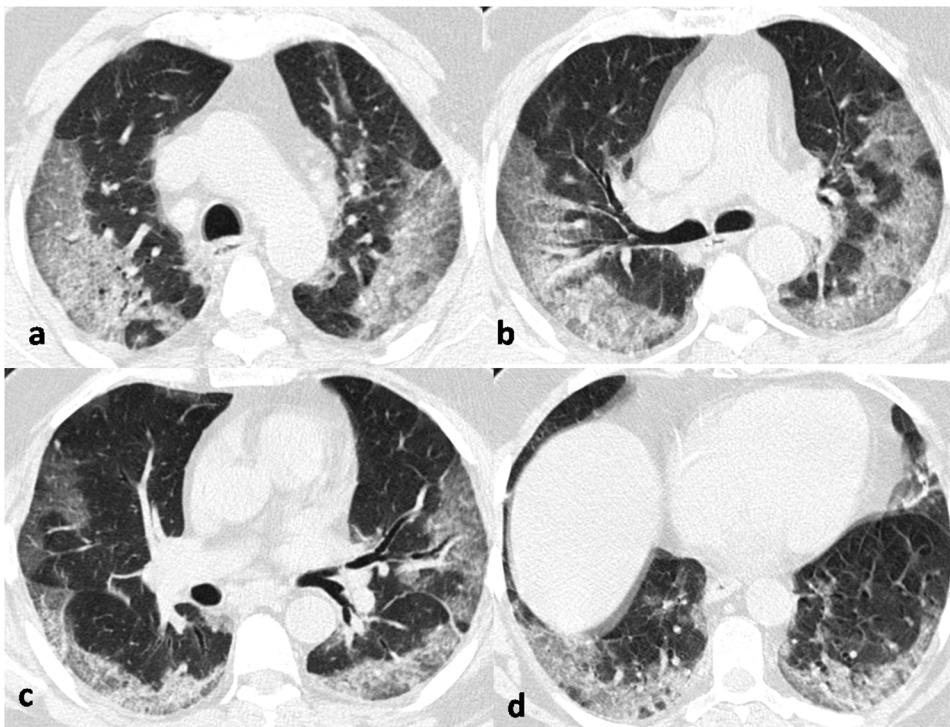
Fig. 2. Non-contrast axial chest CT images in the lung window setting of a 65-year old male COVID-19 positive patient, obtained 7 days after symptom onset, at the carinal (a), sub-carinal (b), mid-basal (c) and basal (d) levels showing bilateral elongated, confluent ground glass opacities with pronounced peripheral and posterior distribution with interlobular septal thickening producing crazy-paving pattern with early progression to consolidation formation.
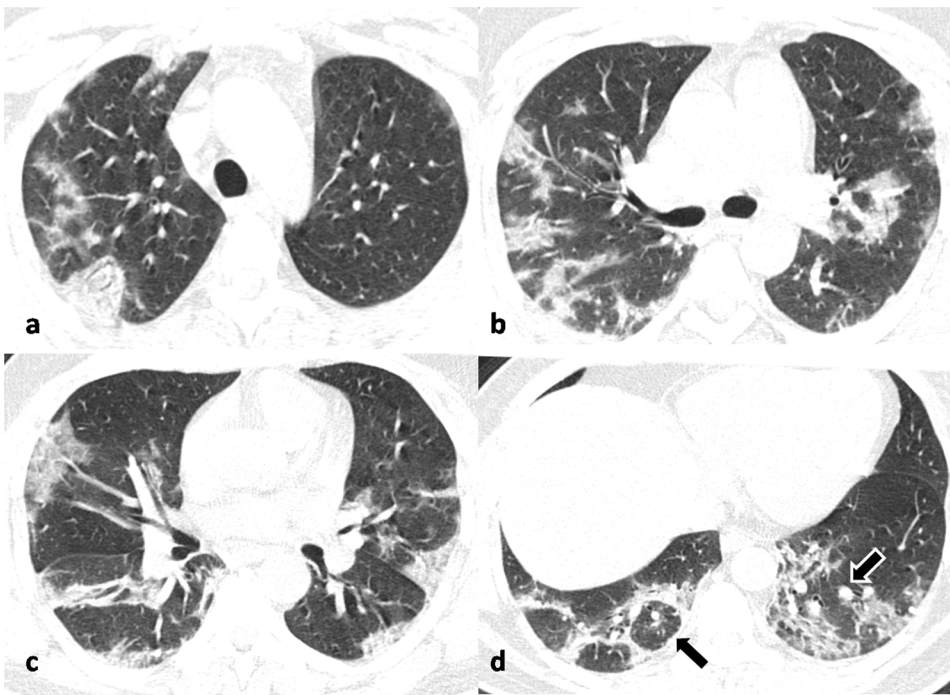

Fig. 3. Non-contrast axial chest CT images in lung window settings of a 40-year old male COVID-19 positive patient, obtained 8 days after symptom onset, in cranio-caudal sequence (a,b,c,d) showing multiple patchy peripheral predominantly posterior ground glass opacities with progression to consolidation in both lungs. There is also evidence of atoll sign in right lung (d) marked by black arrow and perilesional vessel enlargement in left lung (d) marked by black arrow with white border.

4. Discussion

Chest CT manifestations of COVID-19 pneumonia have been widely reported. It has been observed that asymptomatic patients can have a positive chest CT. The converse has also been reported, where symptomatic patients had a negative CT especially during the early phase of the illness [13]. To the best of our knowledge no imaging data of Indian patients is available and majority of the data available have come mostly from China and Europe. A comparison with some severely hit European countries reveals a low case fatality rate (CFR) in Indian patients compared to various European countries which have a higher

CFR. India has recorded 226 770 infections with 6348 deaths as of June 5, 2020 [1]. United Kingdom (281 665 infections; 39 904 deaths), Spain (240 660 infections; 27 133 deaths), Italy (234 013 infections; 33 689 deaths) and France (148 941 cases; 29 007 deaths) have reported almost a similar number of total infections but a much higher number of deaths [1]. However, it is widely cautioned that the actual CFR may be skewed as the estimation of CFR inherently suffers from certain biases. A high proportion of asymptomatic cases in the community may overestimate CFR.

We conducted a prospective study at our CCC to describe the chest CT findings of COVID-19 in our population to gain insight and
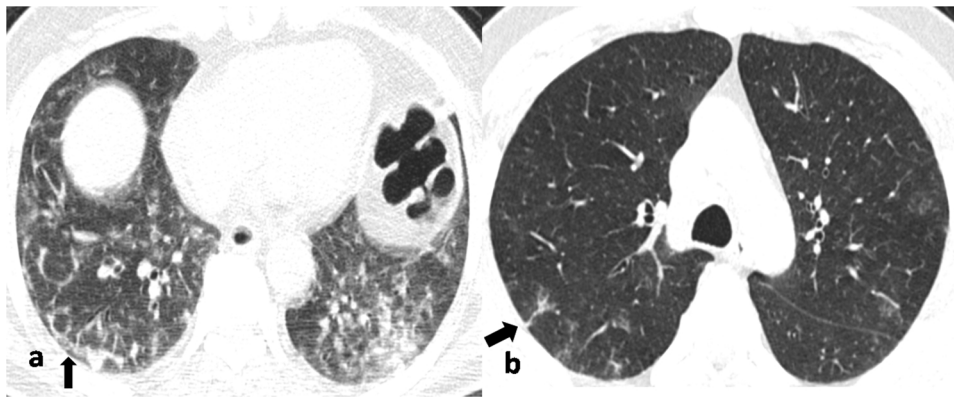
Fig. 4. Non-contrast chest CT axial image (a) in a 62-year old COVID-19 positive male patient, obtained 9 days after symptom onset, showing sub-pleural curvilinear lines (black arrow) with multiple reticulations in right lower lobe and mixed GGO-consolidation pattern in left lower lobe. Fig. 3b in a different 61-year old COVID-19 positive male patient, obtained 6 days after symptom onset, shows evidence of sub-pleural reticulations (black arrow) in the posterior segment of right upper lobe with a few rounded morphology GGOs in left upper lobe.
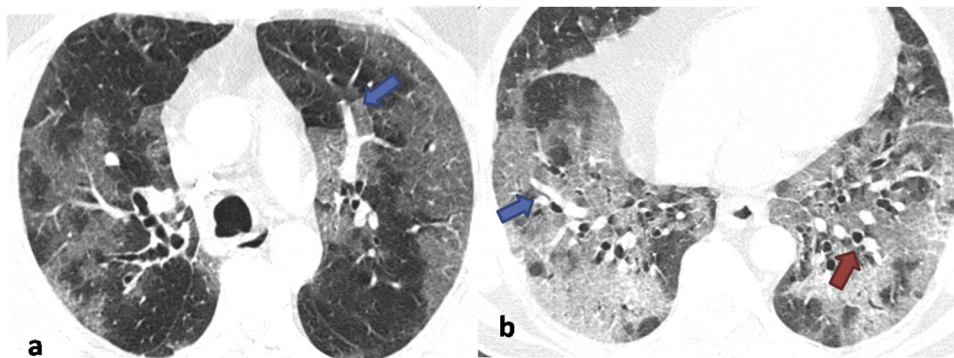

Fig. 5. Non-contrast axial chest CT images in lung window settings of a 62-year old male COVID-19 positive patient, obtained 5 days after symptom onset, showing diffuse ground glass opacities in peripheral and central distribution progressing to frank consolidation in Fig. 2b. There is also evidence of intralesional vessel enlargement (blue arrows in a & b) and bronchial dilatation (red arrow in b).

Table 3
Type of lung opacities and additional findings on CT.

Lung opacity	Number of patients	%
GGO	51	100
Pure GGO	15	29.4
GGO with crazy paving pattern	15	29.4
Pure Consolidation	0	0
Mixed pattern (GGO with consolidation)	21	41.2
Sub pleural linear /curvilinear lines	9	17.6
Nodules	3	5.9
Reticulations	15	29.4
Halo sign	0	0
Reverse Halo sign	9	17.6
Cavitation	0	0
Perilesional /Intralesional vessel enlargement	36	70.6
Bronchial wall thickening	6	11.9
Bronchial dilatation	3	5.9
Air bronchogram sign	12	23.5
Air bubble sign	3	5.9
Additional findings		
Pleural effusion	0	0
Pericardial effusion	0	0
Mediastinal lymphadenopathy	0	0
Findings of existing lung disease		
Emphysema	3	2.5
Sequelae of old healed tuberculosis	18	15.5
Fibrosis/ Interstitial Lung Disease	1	0.8

GGO-Ground glass opacity.

familiarize our radiologists and clinicians with the wide gamut of imaging findings in COVID-19 infected patients in Indian population.

We recorded a negative CT in a high proportion (96/147; 65.3 %) of patients with RT-PCR confirmed SARS-CoV-2. This data is in stark contrast to the studies from China, Korea and Europe which have reported lung parenchymal abnormalities in 61%–100% RT-PCR positive patients [14–16].

Li K et.al [15] reported a CT positivity rate of 71.8 % in confirmed

COVID-19 cases with clinical symptoms. There were 30.8 % mild, 59 % common and 10.2 % severe-critical illness cases, respectively in this study.

Caruso D et.al [17] reported pulmonary findings in 96.6 % of symptomatic cases on CT. Fever (61 %) was the commonest symptom in their cohort followed by cough (56 %) and dyspnea (33 %).

Yu M et.al [18] reported a CT positivity rate of 100 % in their study cohort in which approximately two third of the cases were having mild symptoms with fever in 86 % and dyspnea in 10 %.

In an environmentally homogenous cohort (Diamond Princess Cruise ship), Inui S et.al [13] reported a normal chest CT in 21 % of symptomatic COVID-19 cases with cough (20 %), fever (11 %) and dyspnea (3%). They further observed that nearly half (54 %) of the asymptomatic cases had an abnormal CT. In contrast, nearly two-third of the cases in our study with varying severity of symptoms had a normal CT.

Ai T et.al [19] reported CT findings in 888 (88.7 %) among the total study population of 1014 COVID-19 patients. They further observed that 3% RT-PCR positive cases with clinical symptoms had a normal CT scan.

Bao C et.al [20] in a meta-analysis of 13 studies with 2378 COVID-19 cases found a pooled positive rate of 89.7 % for CT.

The low prevalence of CT findings in laboratory confirmed symptomatic SARS-CoV-2 patients in our population compared to the reported data from other countries raises the possibility of divergent course of the disease in different populations. Putatively, five factors in isolation or in varying combinations could account for this discrepancy.

First, a low prevalence of abnormal CT scans in our population may be because CT scans were performed in all symptomatic RT-PCR positive SARS-CoV-2 patients regardless of the severity of symptoms, with most patients having a mild illness.

Second, a low prevalence of comorbidities in our study cohort with no known immune compromised patients (like cancer patients on chemotherapy) may have contributed to low CT positivity rate. Comorbid illnesses are known to be associated with increased severity of

COVID-19 disease [21].

Third, it may be a consequence of relatively young population in our study with mean age of 40.9 years. However, a comparison between various reported data reveals that many studies which have reported a high CT positivity for COVID-19 had almost a similar age group (< 50 years) [20]. However, some studies had clearly an older study population (> 50 years) [12,17].

Alternatively, it may be reflective of a less severe form of the disease in our population which is tentatively indicated by low CFR in our population so far. The less severity of the disease may in turn result from a less virulent strain of virus or a robust immune status of the population. However, both these presumptive explanations must be viewed with caution and are subject to confirmation by appropriate studies.

One may also argue that some patients with an initial negative CT may have developed lung changes subsequently during the course of illness. The lack of follow-up imaging precludes us from conclusively refuting this possibility. However, the percentage of patients showing respiratory worsening during the hospital stay from the negative CT group may at least indirectly indicate the proportion of patients developing significant lung changes during the hospital stay. Among the patients with a negative initial CT, only one patient presented respiratory worsening during the hospital stay. Bernheim et.al [22] reported 56 % patients imaged within the first 2 days of symptom onset with a negative CT. But only 9% of patients imaged 3–5 days after symptom onset had a normal CT. This number further reduced to 4% when the imaging was performed 6–12 days after symptom onset. We imaged patients after a mean of 5.8 days (range 3–9 days) after the symptom onset.

Among the patients with lung parenchymal abnormalities on chest CT, bilateral and multilobar distribution of pulmonary opacities with a peripheral predilection was commonly observed. Our results fairly corroborate the distribution and type of pulmonary opacities reported in COVID-19 pneumonia.

GGO in the form of pure GGO (29.4 %), GGO with superimposed crazy paving pattern (29.4 %) or GGO admixed with consolidation (41.2 %) was the most dominant lung parenchymal abnormality encountered in all the cases. These findings are in concordance with the multiple studies summarized in the systematic review by Salehi et al. [23] wherein they found that GGO was present in 88 % cases across 22 studies reported from various countries.

The intriguing finding of segmental or subsegmental intra-lesional or peri-lesional pulmonary vessel enlargement was observed in 70.6 % patients. Our findings are in concurrence with Yan Li et al. [24] who reported vascular enlargement in 82.4 % and Caruso D et al. [17] who reported vessel enlargement in 89 % patients. The various putative etiologies that have been put forth to account for this unique finding of vascular enlargement include, vasodilatation induced by the release of proinflammatory cytokines, small vessel pulmonary embolism and infection induced pulmonary vasculitis [25]. The finding of pulmonary vascular enlargement seems to have a diagnostic value as it has not been reported previously in any infectious disease settings. Bai et al. [26] reported vascular enlargement to be frequently associated with COVID-19 pneumonia compared to non−COVID-19 pneumonia with a significant p-value (< 0.001). The presence of enlarged vessel sign may help discriminate COVID-19 pneumonia from non−COVID-19 pneumonia.

The percentage of the diseased lung was higher in patients with severe disease (29.6 ± 12.3 %) compared to the patients with a mild form of disease (10.2 ± 6.6 %). However, the small number of patients with severe disease precluded us from performing a meaningful correlation analysis within the subsets.

CT is not recommended as a screening tool for the diagnosis of COVID-19 [27,28]. However, CT has contributed to the clinical management of the COVID-19 disease and in our understanding of the disease. According to the German Radiological Society, CT may aid in assessing the initial extent of the lung involvement, help in recognition of the pneumonia-associated complications and also help in monitoring the progression of the disease in severe cases [27]. According to American College of Radiology (ACR) guidelines, CT should be reserved for hospitalized, symptomatic patients with specific clinical indications like worsening respiratory status [28]

There are several limitations to our study. First, we focused on initial or baseline CT findings and did not perform follow-up CT examinations. This may result in non-inclusion of symptomatic cases that may have developed lung changes late in the course of disease and hence a spurious high rate of negative CTs in the study population. Second, there may have been a selection bias as imaging was performed in all symptomatic cases regardless of the severity of illness. The small size of study population is also a limitation.

5. Conclusion

In conclusion, we found a high proportion (65.3 %) of normal chest CTs in mildly symptomatic laboratory-confirmed SARS-CoV-2 patients. Patients with a positive CT showed the same CT features as reported in other series with a predominance of GGOs in a bilateral and multilobar distribution with posterior and peripheral predilection.

Funding

CRediT authorship contribution statement

Arshed Hussain Parry: Conceptualization, Methodology, Validation, Formal analysis, Resources, Investigation, Writing - original draft, Writing - review & editing, Supervision. **Abdul Haseeb Wani:** Conceptualization, Methodology, Validation, Formal analysis, Resources, Investigation, Writing - original draft, Writing - review & editing, Supervision. **Mudasira Yaseen:** Conceptualization, Methodology, Validation, Formal analysis, Resources, Investigation, Writing - original draft, Writing - review & editing, Supervision. **Khurshid Ahmad Dar:** Methodology, Validation, Resources, Formal analysis. **Naseer Ahmad Choh:** Methodology, Validation, Formal analysis. **Naseer Ahmad Khan:** Methodology, Validation, Formal analysis. **Naveed Nazir Shah:** Methodology, Validation, Formal analysis. **Majid Jehangir:** Methodology, Validation, Formal analysis.

Declaration of Competing Interest

None.

References

[1] World Health Organization, Coronavirus Disease 2019 (COVID-19): Situation Report, (2020) 137.

[2] Y. Chen, L. Li, SARS-CoV-2: virus dynamics and host response, Lancet Infect. Dis. (March) (2020).

[3] C. Huang, Y. Wang, X. Li, et al., Clinical features of patients infected with 2019 novel coronavirus in Wuhan, China, Lancet 395 (10223) (2020) 497–506, https://doi.org/10.1016/s0140-6736(20)30183-5.

[4] W.H. Kong, Y. Li, M.W. Peng, D.G. Kong, X.B. Yang, L. Wang, M.Q. Liu, SARS-CoV-2 detection in patients with influenza-like illness, Nat. Microbiol. (April) (2020) 1–4.

[5] Y. Yang, M. Yang, C. Shen, et al., Evaluating the Accuracy of Different Respiratory Specimens in the Laboratory Diagnosis and Monitoring of the Viral Shedding of 2019-nCoV Infections, (2020), https://doi.org/10.1101/2020.02.11.20021493.

[6] A.H. Parry, A.H. Wani, Pulmonary embolism in coronavirus disease-19 (COVID-19) and use of compression ultrasonography in its optimal management, Thromb. Res. (May) (2020).

[7] M. Chung, A. Bernheim, X. Mei, et al., CT imaging features of 2019 novel coronavirus (2019-nCoV), Radiology (2020) 200230, , https://doi.org/10.1148/radiol.2020200230.

[8] A. Bernheim, X. Mei, M. Huang, et al., Chest CT findings in coronavirus Disease-19 (COVID-19):relationship to duration of infection, Radiology (2020) 200463, , https://doi.org/10.1148/radiol.2020200463.

[9] World Health Organization, Clinical Management of Severe Acute Respiratory Infection When Novel Coronavirus (nCoV) Infection Is Suspected: Interim Guidance, (2020) https://www.who.int/publications-detail/clinical-management-of-severe-acute respiratory-infection-when-novel-coronavirus-(ncov)-infection-is-suspected. Published on January 12, 2020. Updated on March 13, 2020. Accessed on March 20, 2020.

[10] S. Ruggiero, G. Weisser, Integrating Mac systems into a medical IT infrastructure, White paper (2007).

[11] D.M. Hansell, A.A. Bankier, H. MacMahon, T.C. McLoud, N.L. Muller, Remy J. Fleischner Society, Glossary of terms for thoracic imaging, Radiology 246 (March (3)) (2008) 697–722.

[12] S.M. Tabatabaei, H. Talari, F. Moghaddas, H. Rajebi, Computed tomographic features and short-term prognosis of coronavirus disease 2019 (COVID-19) pneumonia: a single-center study from Kashan, Iran, Radiology 2 (April (2)) (2020) e200130.

[13] S. Inui, A. Fujikawa, M. Jitsu, N. Kunishima, S. Watanabe, Y. Suzuki, S. Umeda, Y. Uwabe, Chest CT findings in cases from the cruise ship "Diamond Princess" with coronavirus disease 2019 (COVID-19), Radiology 2 (March (2)) (2020) e200110.

[14] Z. Ye, Y. Zhang, Y. Wang, et al., Chest CT manifestations of new coronavirus disease 2019 (COVID-19): a pictorial review, Eur. Radiol. (2020), https://doi.org/10.1007/s00330-020-06801-0.

[15] K. Li, Y. Fang, W. Li, C. Pan, P. Qin, Y. Zhong, X. Liu, M. Huang, Y. Liao, S. Li, CT image visual quantitative evaluation and clinical classification of coronavirus disease (COVID-19), Eur. Radiol. (March) (2020) 1-0.

[16] Y. Li, L. Xia, Coronavirus Disease 2019 (COVID-19): role of chest CT in diagnosis and management, Am. J. Roentgenol. (February) (2020) 1–7.

[17] D. Caruso, M. Zerunian, M. Polici, F. Pucciarelli, T. Polidori, C. Rucci, G. Guido, B. Bracci, C. de Dominicis, A. Laghi, Chest CT features of COVID-19 in Rome, Italy, Radiology (April) (2020) 201237.

[18] M. Yu, D. Xu, L. Lan, M. Tu, R. Liao, S. Cai, Y. Cao, L. Xu, M. Liao, X. Zhang, S.Y. Xiao, Thin-section chest CT imaging of coronavirus disease 2019 pneumonia: comparison between patients with mild and severe disease, Radiology 2 (April (2)) (2020) e200126.

[19] T. Ai, Z. Yang, H. Hou, C. Zhan, C. Chen, W. Lv, Q. Tao, Z. Sun, L. Xia, Correlation of chest CT and RT-PCR testing in coronavirus disease 2019 (COVID-19) in China: a report of 1014 cases, Radiology (February) (2020) 200642.

[20] C. Bao, X. Liu, H. Zhang, Y. Li, J. Liu, Coronavirus disease 2019 (COVID-19) CT findings: a systematic review and meta-analysis, J. Am. Coll. Radiol. (March) (2020).

[21] F. Zhou, T. Yu, R. Du, G. Fan, Y. Liu, Z. Liu, J. Xiang, Y. Wang, B. Song, X. Gu, L. Guan, Clinical course and risk factors for mortality of adult inpatients with COVID-19 in Wuhan, China: a retrospective cohort study, Lancet (March) (2020).

[22] A. Bernheim, X. Mei, M. Huang, Y. Yang, Z.A. Fayad, N. Zhang, K. Diao, B. Lin, X. Zhu, K. Li, S. Li, Chest CT findings in coronavirus disease-19 (COVID-19): relationship to duration of infection, Radiology. (February) (2020) 200463.

[23] S. Salehi, A. Abedi, S. Balakrishnan, A. Gholamrezanezhad, Coronavirus disease 2019 (COVID-19): a systematic review of imaging findings in 919 patients, Am. J. Roentgenol. (March) (2020) 1–7.

[24] Y. Li, L. Xia, Coronavirus disease 2019 (COVID-19): role of chest CT in diagnosis and management, Am. J. Roentgenol. (March) (2020) 1–7.

[25] A.H. Parry, A.H. Wani, Segmental pulmonary vascular changes in COVID-19 pneumonia, Am. J. Roentgenol. (May) (2020) W1-.

[26] H.X. Bai, H. Hsieh, Z. Xiong, K. Halsey, J.W. Choi, T.M. Tran, I. Pan, L.B. Shi, D.C. Wang, J. Mei, X.L. Jiang, Performance of radiologists in differentiating COVID-19 from viral pneumonia on chest CT, Radiology (March) (2020) 200823.

[27] J. Vogel-Claussen, J. Ley-Zaporozhan, P. Agarwal, J. Biederer, H.U. Kauczor, S. Ley, H. Kühl, U.G. Mueller-Lisse, T. Persigehl, C.L. Schlett, D. Wormanns, Recommendations of the Thoracic Imaging Section of the German Radiological Society for Clinical Application of Chest Imaging and Structured CT Reporting in the COVID-19 Pandemic, InRöFo-Fortschritte auf dem Gebiet der Röntgenstrahlen und der bildgebenden Verfahren, © Georg Thieme Verlag KG, 2020 May 26.

[28] https://www.acr.org/Advocacy-and-Economics/ACR-Position-Statements/Recommendations-for-Chest-Radiography-and-CT-for-Suspected-COVID19-Infection. Accessed 25/05/2020.